INVESTIGATION OF EROSION AND PRESSURE FOR DIRECT AND INDIRECT ACOUSTIC CAVITATION TESTING

[1]Jonty Mago,[2]Sandeep Bansal,[3]Dheeraj Gupta, [4]Vivek Jain
[1]M.E Student,[2]PhD Research Scholar,[3]Associate Professor, [4]Associate Professor
[1]Mechanical Engineering Department,
[1]Thapar Institute of Engineering & Technology, Patiala, India.

Abstract : In the present work, investigation for erosion and pressure by direct and indirect vibratory cavitation testing of the austenitic stainless steel 316 has been performed. Both Specimens are exposed for cavitation erosion on vibratory cavitation apparatus (probe sonicator) of frequency 20 kHz at amplitude 60µm for 180 minutes. The surfaces of the fractured specimens are examined with scanning electron microscopy and surface profilometer. For the acoustic pressure computation, ANSYS 19.2 has been utilised to model and simulate the actual experimental conditions in harmonic response module, in addition, the ACT (ANSYS Customization Toolkit) of ExtAcoustic and ExtPiezo has been used. Cumulative volume loss in direct vibratory cavitation testing is found to be three times more as compared to indirect vibratory cavitation testing. An SEM images reveals that deep craters and excessive pits are formed in case of specimens are tested via direct vibratory cavitation method. Measured Rq values are 3.18µm and 2.83 µm in direct and indirect vibratory cavitation testing, respectively. Higher Rq value confirmed that more severe fracture occurred on specimens tested with the direct method. More negative acoustic pressure in direct method (320210 pa) validate the reason for higher damage, less probability of bubbles escape, and more microjets formation as compared to the indirect method (74964 pa). The negative acoustic pressure in the direct method is approx. 4 times more than in an indirect method.

Index Terms **- ANSYS 19.2, ASTM G32-16, Acoustic Pressure, Cavitation Erosion, Optical Micrographs, Volume Loss**

I. INTRODUCTION

Cavitation erosion is the most common type of surface degradation process occurs in the components of the hydropower plants [1]. However, it happens due to sudden fluctuation in the pressure in the flowing liquid. At the boundaries when the pressure of the flowing liquid falls below its vapour pressure, the formation of empty cavities known as bubbles takes place [2]. Further, when the pressure starts rising, the growth of the bubbles start reversing, and at high pressure, it collapses. This collapsing process generates the shock waves and microjets repeatedly, which exert tremendous stresses on the surface of the components. This ultimately led to surface fatigue, material removal, and pit formation. In the end, the functionality of the component is completely lost [3]. Most commonly used materials in hydropower plants components are austenitic and martensitic stainless steel. Due to their less hardness, they are more susceptible to cavitation [4]. In the last two decades, the researchers have worked on enhancing the cavitation resistance of the material either by replacing the existing component with the more cavitation resistant materials or by just coating/cladding the surface of the component which is more prone to cavitation damage [5]. For the research purpose, many testing methods and rigs have been developed to mimic the real cavitation condition. So that comparison has been carried out between materials and surface coating/cladding developed for the cavitation erosion resistance and its degradation phenomena [6]. There are four types of methods that are used for the cavitation testing, which are vibratory apparatus, cavitation liquid jets, cavitation tunnels, and rotating disc apparatus [7].

All methods mentioned above generate different type of cavitation conditions like cavitation liquid jets, and cavitation tunnel generate travelling bubble cavitation. Whereas the rotating disc apparatus generates vortex cavitation and vibratory apparatus generates attached cavity cavitation [8]. Repeatability of the testing apparatus is the main factor for the selection of cavitation testing rig. Other important factors for the selection of cavitation rig are sample shape and size. Whereas in the rotating disc apparatus several disadvantages like standardized position and rotational velocity of the sample are not done yet, and almost two times the size of vibratory cavitation apparatus [9-10]. In the case of cavitation tunnel, many factors which affect the cavitation erosion like the shape of the flow geometry, velocity & pressure of the fluid and standard value of both pressure and velocity are not available in the literature [11-12]. Therefore, vibratory apparatus (Also known as acoustic cavitation apparatus) and cavitation liquid jet system are standardized by the American society of testing methods (ASTM) in the ASTM G32-16 (its earlier version is known as G32-10) and G-134-17(its more previous version is known as G134-95) respectively [13-14].

Moreover, these methods are most commonly used due to their less sophisticated & smaller apparatus. In the case of materials and surface coatings/cladding comparative studies, ASTM G32-16 is the most preferred in literature [15-17]. In ASTM G32-16, the standard diameter & thickness of the sample, vibratory amplitude, specimen vibration frequency, test liquid, and its container are specified [13]. In this method the sample is attached to the ultrasonic horn with the screw threads which must be the integrated part of the sample and when horn vibrates (accelerate, decelerate) about its mean position that produces the vapour bubbles due to sudden change in pressure and bubbles collapsesnear to the surface of the material, generates micro jets and causes erosion [18].

In some cases like hard composite coating/cladding, it's difficult to develop screw thread type of samples. So, the researcher has introduced the amendment in G32-16 (Indirect Method). Instead of attaching the specimen with the horn, the specimen is placed opposite to the tip of the horn and stream of the bubble is ejected towards the surface of the material and when it explodes, it generates impact force on the surface of the material and causes stress generation as well as material removal [19-21]. Due to more simplicity, the G32-16 with the amendment is frequently used in the field of cavitation resistance coatings/claddings. As the researcher mentioned, cavitation is not only single phenomena, even pH level of water (corrosion) and silt content in water also responsible for enhancing the cavitation effect by making the material more prone to cavitation damage [6]. ASTM G32-16

(Indirect Method) gives the more provision of testing the combined result of cavitation, corrosion, and silt erosion by just adding acid or base and silt particle to the test liquid [22-23].

Whereas it has been reported that in direct method bubbles cloud collapses in a hemispherical way and indirect method, bubbles cloud collapses in a cylindrical way [24-28]. Also, in the case of Aluminium alloy Al-7075 is has been reported that cylindrical collapsing causes less material erosion as compared to hemispherical bubbles cloud collapse [29]. The disadvantage of the indirect method is that the additions of other mandatory test parameters, i.e., stand-off distance and immersion depth of specimen. In a few indirect cavitation parametric studies, it has been concluded that bubbles collapsing impact force decreases with an increase in stand-off distance, increase with the increase in amplitude and decrease with an increase in immersion depth [30]. Pressure sensors are also being utilized in some studies to measure the impact force produced by the cavitation jet apparatus and vibratory cavitation apparatus, but the sensors are protected with other materials to avoid cavitation that may give erroneous readings [31-32].

Further, few mathematical modelling and simulation studies have been done [33]. Also, simulation results can provide more information at less cost and material wastage. Due to very few comparative studies reported for direct and indirect acoustic cavitation [34]. The scope of current work is an investigation of the cumulative volume loss due to cavitation erosion in material and acoustic pressure generated in test liquid in direct and indirect acoustic cavitation for stainless steel SS316L. The acoustic pressure variation in direct and indirect acoustic cavitation has been studied by simulation using ANSYS 19.2 in harmonic response module. The fractographic analysis of eroded specimen has been carried out using a secondary electron imaging in scanning electron microscopy (SEM).

II. EXPERIMENTATION

2.1Material Details

For the present examination, Stainless steel 316L Grade has been selected. Because of its slightly better properties than 300 series family most commonly used grade 304. SS316L have 2-3% of Molybdenum, which provides excellent resistance to a highly corrosive environment. Procured material was characterised to determine its metallurgical and mechanical properties. From the optical micrograph in figure 1 (a), it is visible that material has a grain structure of pure austenitic stainless steel. Whereas an austenitic grain has a greyish appearance and ferrite grains are tannish in colour. The average grain size is measured by using Micro Cam 4.0 (Microstructure Image Analyzing Software Make: Radical Scientific, India). Method used for grain size measurement is ISO 643 (Equivalent to ASTM E112-13 [35]) as shown in figure 1 (b). The average grain size of material came out to be approx. 30µm. Microhardness of the material is monitored by using Vicker's microhardness tester (Make: MetaTech). The average value of microhardness of material is 180±20 HV. The spectrometer (Make: Foundry Master) was utilized to determine the elemental composition of the material. The obtained elemental composition of the material is tabulated in table 1.

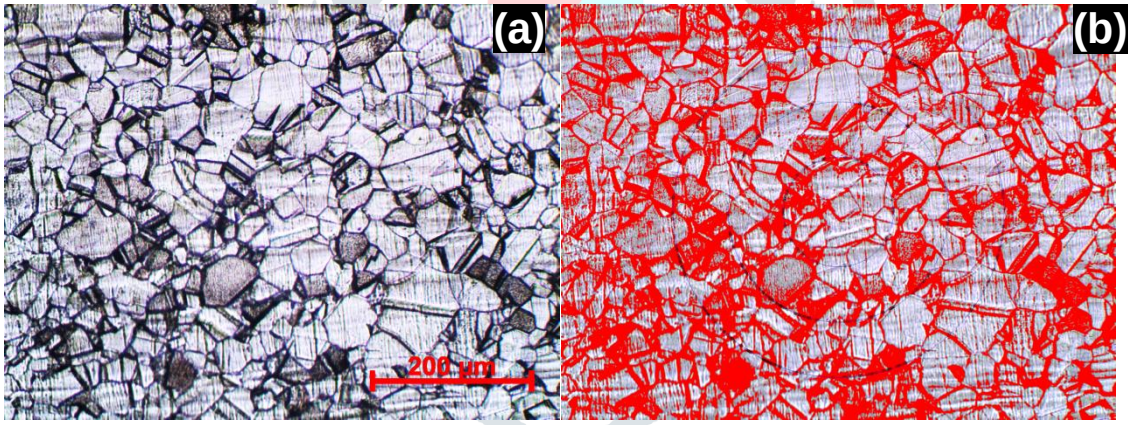

Fig. 1: Optical Micrographs of (a) Grain Structure of SS-316L (b) Grain size Measurement of SS316L in Micro Cam 4.0 (c) Indentation geometry

Table 1. The Elemental Composition of Stainless Steel-316L

Chemical Elements								
C	P	S	Si	Mn	Mo	Ni	Cr	Fe
0.0243	0.041	0.06	0.281	1.26	2.07	10.2	17.1	Bal.

2.2 Experimental Cavitation Erosion Testing

Square sample of area 15*15 mm & thickness 6 mm is used as specimens for the cavitation erosion testing. The samples are polished up to 0.2 µm Rq (mean square roughness) value, as mentioned in the ASTM G32-16 the Rq value of the surface before testing must be less than 0.8 µm. The polishing process carried out by using embry papers starting from grade 100, followed by 200, 600, 800, 1000, 1200, 1500, 2000, 2500, and 3000 (50 stokes each). In the end, the specimens are polished by using a diamond polishing paste of 1µm on rotating disc polisher for 10 minutes. After polishing, specimens are tested using probe sonicator (Make: Kamtronics Technology Pvt. Ltd.) for direct and indirect acoustic cavitation (Bubbles generation via ultrasonic

vibrations). Schematic of direct and indirect acoustic cavitation is shown in Figure2 (a) & (b) respectively and Actual Probe Sonicator for cavitation erosion testing is shown in Figure3. Cavitation test parameters were selected based on literature and standards, i.e., used for both actual & simulation purposes are summarized below in table 2. Test runs for each specimen is 3 hours and mass loss in the specimens due to cavitation erosion has been measured after the interval of every half an hour using the weighing balance of least count 0.1 mg (Make: CAS global, Model: CAS220).

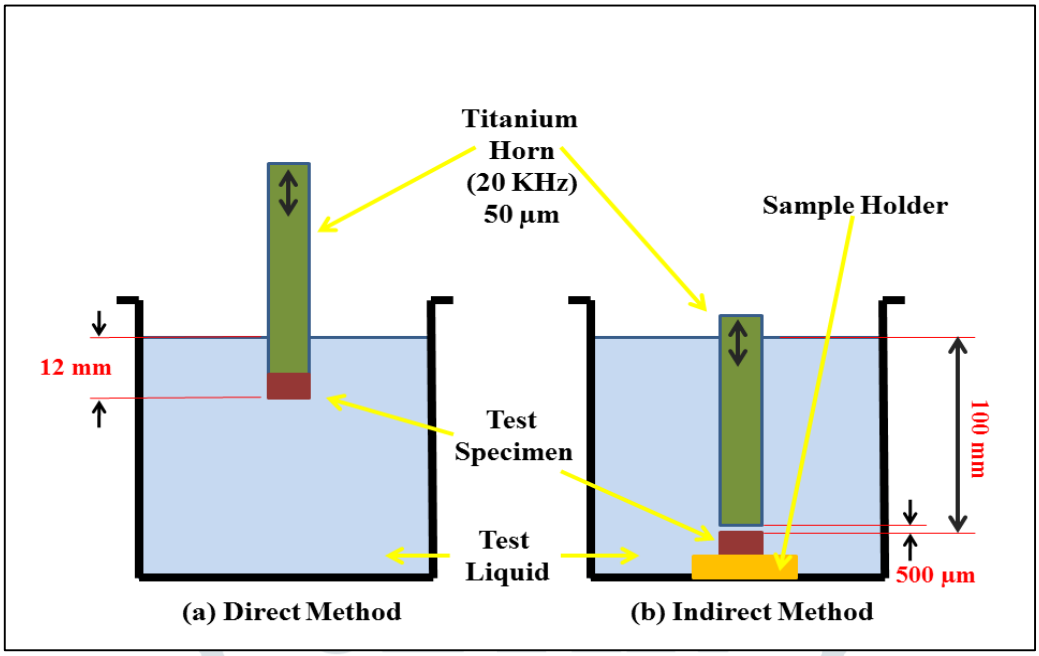

Fig.2: The Schematic of (a) Direct Acoustic Cavitation (b) Indirect Acoustic Cavitation

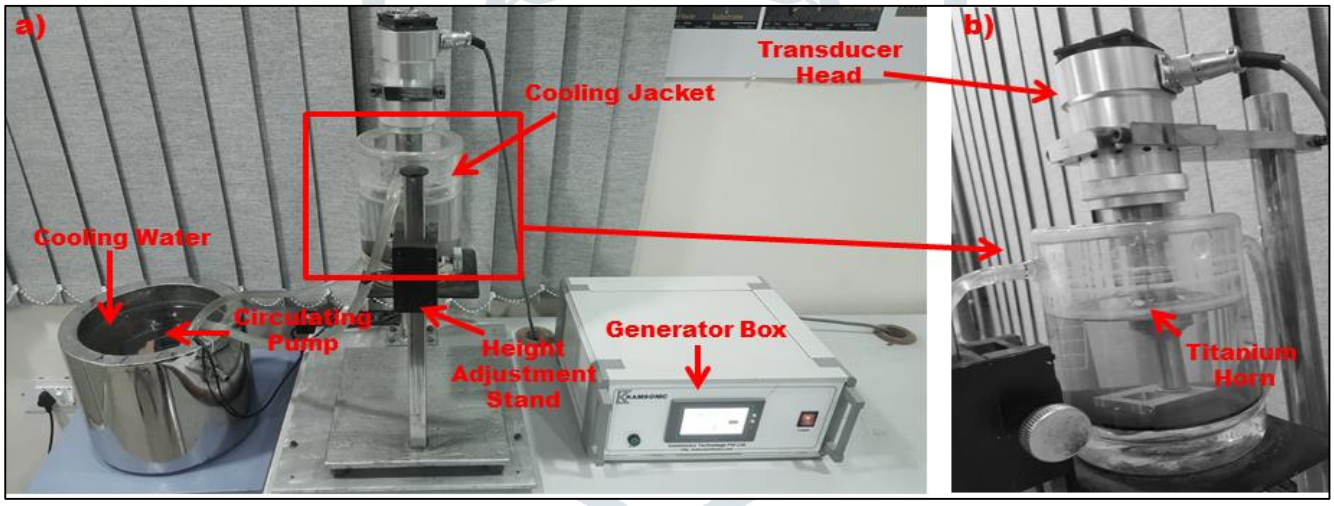

Fig 3: The Actual Setup of (a) Cavitation Probe Sonicator (b) Titanium Horn & Transducer Head Assembly

2.3 Acoustic Cavitation Simulation

To find out the acoustic pressure produced in direct and indirect vibratory cavitation. The actual experimental conditions need to be replicated in the simulation software. First of all, the CAD model of the exact experimental setup has been made in the ANSYS 19.2 design modeller. For current simulation, the horn of 15 mm diameter and 45 mm length has been made in design modeller & final CAD model for direct and indirect cavitation testing setup has been illustrated in Figure4 (a) & (b) respectively. After the successful development of the CAD model, the material properties have been added in the engineering database. Material properties used for present was gathered from material testing (Steel and water) and similar kind of setups mentioned in the literature [36]are mentioned in table 3. Next step is to assign the material properties to various components in the mechanical model. The sample is of stainless steel, the horn is of titanium alloy, the vibration sensor is of a piezoelectric crystal, and the test liquid is distilled water. The fourth step is mesh generation, whereas, in the current study, ANSYS 19.2 default (automatic) mesh is considered. CAD Model for direct and indirect has been divided into 11550 nodes & 5693 elements and 15834 nodes & 8128 elements, respectively while meshing. The CAD models after meshing are shown in figure 4 (c) & (d). In the end, the constraints are applied to the CAD model. The fixed constraint is applied to the top end of the static load, and the fixed voltage is assigned to the piezoelectric sensor for the output of the required amplitude. For the current experiment, 42.23 Volt is given to the sensor because that voltage is computed from the actual experimental setup. The actual setup produces 60±2µm amplitude corresponding to 114.390 Watt power and 0.324-ampere current. After that final simulation run for acoustic pressure and amplitude output corresponding to every node and elements has been carried out. Results are computed in the harmonic response module; in addition, the ACT (ANSYS Customization Toolkit) of ExtAcoustic and ExtPiezo has been used. The details of equations and

method used for analyzing the FE Model at the software background in harmonic response module for calculation of acoustic pressure and amplitude are explained by the author [36].

Table 2. Cavitation Test Parameters for Actual Experiment and Simulation

Test Parameters	Description	
	Direct Cavitation	Indirect Cavitation
Sample location	Attached with horn tip	Facing to horn tip
Immersion Depth of Sample (mm)	12	100
Stand of Distance (SOD-µm)	-	500
Amplitude (µm)	60±2	60±2
Frequency (kHz)	20±0.1	20±0.1
Horn Tip Diameter (mm)	15	15
Test Liquid	Distilled water	Distilled water
Temperature of Test liquid (°C)	25±2	25±2
Ambient Temperature (°C)	22±2	22±2

Table 3. Physical Properties of the Materials Used

Properties	Materials			
	Stainless Steel	Titanium Alloy	Piezoelectric Material	Distilled Water
Density (Kg/m^3)	7890	4510	7210	1000
Elastic Modulus (GPa)	190	105	**	-
Poisson's Ratio	0.3	0.37	**	-
Speed of Sound in Medium(m/s)	5188	4920	3463	1500

**Piezoelectric Material is Anisotropic Material. Hence, for the piezoelectric, there is a separate elastic constants matrix shown below in Table 4.

Table 4. Values of Elastic Constant for Piezoelectric Material

D[*,1]Pa	D[*,2]Pa	D[*,3]Pa	D[*,4]Pa	D[*,5]Pa	D[*,6]Pa
1.5e+011	-	-	-	-	-
8.6e+010	1.35e+011	-	-	-	-
8.2e+010	8.6e+010	1.53e+011	-	-	-
0	0	0	2.9e+010	-	-
0	0	0	0	2.9e+010	-
0	0	0	0	0	3.5e+010

III. Results & Discussion

3.1 Cavitation Erosion Wear Studies

The mass loss of specimen measured on a weighing machine is converted into volume loss after dividing it by material density. And figure 5 the plot presents the relationship between cumulative volume losses in SS316L after specified time duration of direct and indirect cavitation testing. It is visible from the plot that volume loss is almost equal in both of the cases until 30 minutes. However, after another 1 hour, the volume loss in direct cavitation testing is almost 2 times that of indirect cavitation. Whereas after the complete 3 hours testing volume loss in direct cavitation is found to be 3 times more as compared to indirect cavitation testing. However, in literature is being reported that in direct cavitation system bubbles movement towards specimen and microjet strikes at the specimen with more velocity [24]. They concluded that in the first half of the first cycle when horn begins to move downward from the mean position formation of bubbles takes place due to the high velocity of horn and the pressure fell below its vapour pressure and then in the second half of the first cycle horn decelerate and move upward from the mean position. During then pressure falls below vapour pressure in the upper region and lower region pressure became positive due to this the bubbles formed in the first half of the cycle start rising in the test liquid with velocity (Vb-Velocity of the bubble). In the same time, the horn begins moving towards the down position with velocity (Vh-Velocity of the horn). Now here, the concept of relative velocity comes into the picture. According to the concept of relative velocity when two objects were moving towards each other direction, their velocities get added. So the velocities of the bubbles in direct the specimen in case of direct cavitation becomes Vb+Vh. This decrease the probability of bubbles escape, which means the high population of bubbles collapses and more number of microjets hits on the surface of the specimen. Whereas in the case of indirect cavitation, it is approximately equal to Vh only. So that in case of probability bubbles escape is high and fewer microjets hits on the surface of the specimen. Hence, Due to less momentum and less probability in case indirect cavitation, the wear loss in case of indirect cavitation is less.

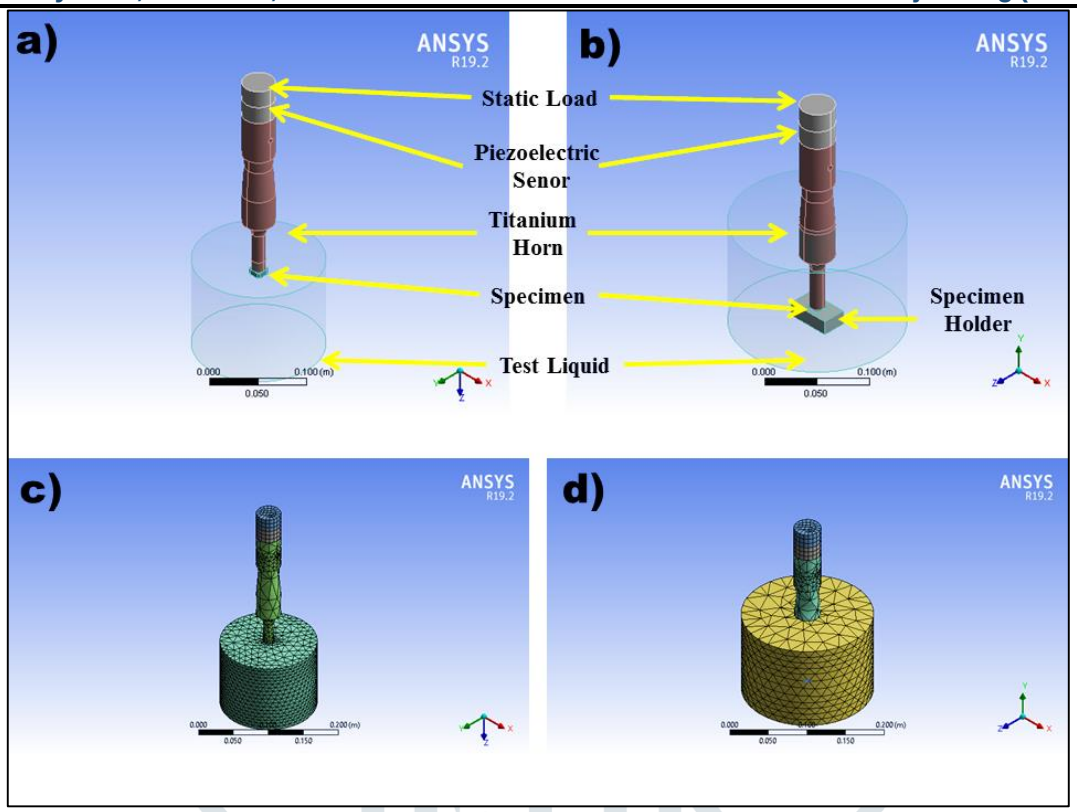

Fig.4: CAD Model of (a) Direct Cavitation Testing Rig (b) Indirect Cavitation Testing Rig
(c) Direct Cavitation Testing Rig After Meshing (d) Indirect Cavitation Testing Rig After Meshing

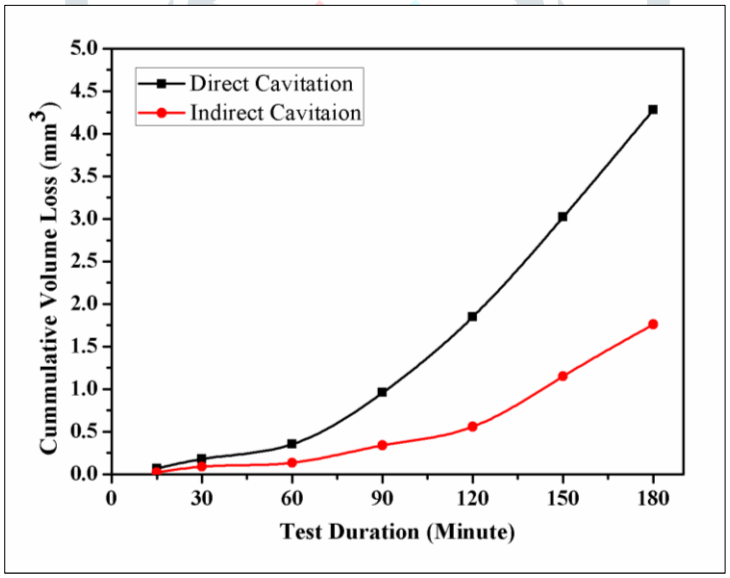

Fig. 5: Cumulative Volume Loss V/S Cavitation Erosion Time

3.2Cavitation erosion Mechanism & Fractographic Analysis

Figure 6 (a), (b) & (c) show the surface of the specimen before testing, after 3 hours of direct vibratory cavitation testing and after 3 hours of indirect vibratory cavitation testing respectively. It is visible that the erosion in direct cavitation more focused at the central region of the specimen. However, erosion in indirect cavitation is equally distributed over the circular region (Approximately equal to the diameter of the titanium horn).

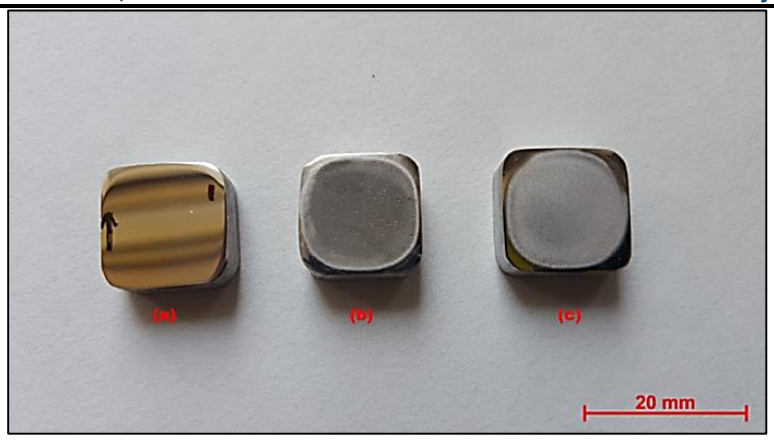

Fig 6: Specimen Top Surface (a) Before Testing (b) After Direct Cavitation Testing (c) After Indirect Cavitation Testing

Figure 7 (a) & (b) shows the SEM micrographs of surface morphology of worn-out materials after direct and indirect cavitation testing. The surface of the specimen after direct vibratory cavitation to be obscured by a large number of deep craters, pits, and microcracks. The presence of these features indicates plastic deformation and surface fatigue as the primary degradation mechanism. Whereas a large number of microspores and pits their locality is covered plastically deformed lips in the grain boundaries region observed on the surface of the specimen after indirect vibratory cavitation. From the SEM micrographs, it has been quickly concluded that the more severe fracture is observed in the case of direct vibratory cavitation because of fewer microjets, less momentum and less bubbles activity. The severity of damage is also confirmed by surface roughness testing by surface profilometer (Make-Mitutoyo, Model-SJ400). As mentioned earlier the roughness of the specimen before testing was 0.2µm whereas after testing specimen losses its luster that appears like a darker in the colour that can be seen in figure 6(b) & 6 (c). Measured roughness (R) profile of specimens before and after testing are shown in figure8 (a), 8(b) & 8(c). However, the deep craters and pits appear in the roughness data. Rq value found to be 3.18 µm and 2.83 µm on specimens surfaces after direct and indirect acoustic cavitation. Higher Rq value in case of direct vibratory cavitation confirms that cavitation damage to the material is more intense in case direct acoustic cavitation.

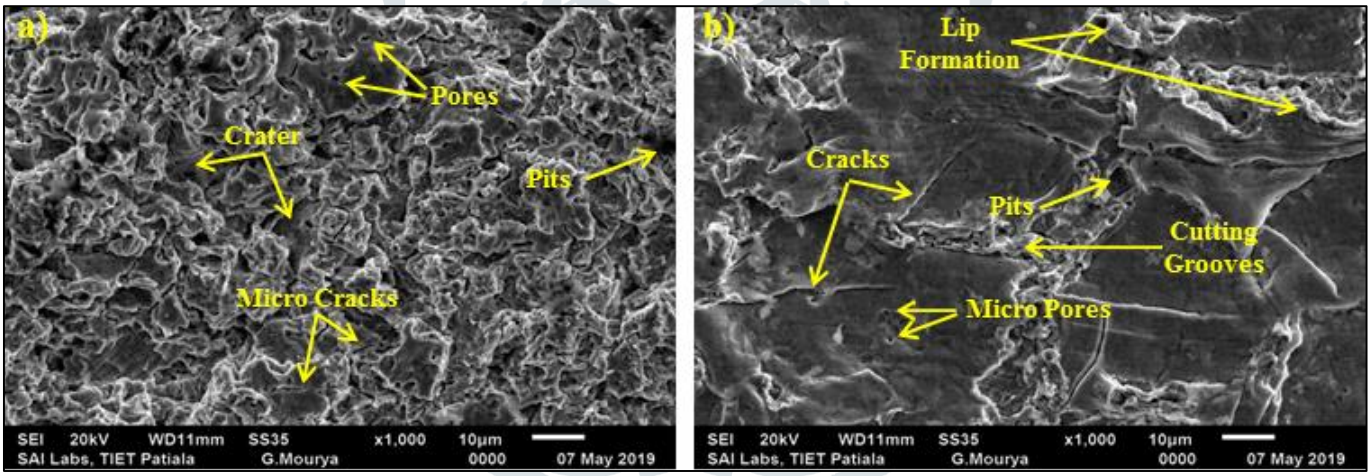

Fig. 7: SEM Micrographs of surface morphology of worn-out materials (a) After Direct Cavitation Testing (b) After Indirect Cavitation Testing

3.3Acoustic Pressure Simulation Results

Figure 9 (a) &10 (a) shows the displacement in ultrasonic horn for direct and indirect method during simulation of actual experimental conditions in ANSYS 19.2. Error in actual and simulation is less than 1 percent. Figure 10 (b) shows the enlarged view of displacement of the ultrasonic horn in the direct method. Whereas figure 9 (b), 9 (c) represent the acoustic pressure generated during upward movement of horn form its mean position & the acoustic pressure generated during downward movement of horn form its mean position respectively in direct vibratory cavitation.Similarly, figure 10 (c), 10 (d) represent the acoustic pressure generated during downward movement of horn form its mean position & the acoustic pressure generated during upward movement of horn from its mean position respectively during indirect vibratory cavitation testing. Hemispherical pressure distribution is visible direct vibratory cavitation test & cylindrical pressure distribution visible in indirect vibratory cavitation, and the same type of bubbles collapse is reported in the literature. In case of direct method minimum and maximum acoustic pressure is found at the middle of the specimen, i.e., the cause more bubbles formation & collapse at that locality. Also, the direct cause of high erosion in the middle of the specimen. Whereas in indirect method minimum and maximum pressure zone forms away from the specimen. However, the pressure is the same at all located above the specimen. That is why the erosion due to cavitation approximately the same at all locations of the specimen. The maximum and minimum pressure in the direct method is 320210 Pa and -320210 Pa, respectively. The maximum and minimum pressure in the indirect method is 74964 Pa and -74964 Pa, respectively. The negative acoustic pressure is approximately four times more while using the direct method. More negative pressure increases the probability of bubbles formation as well as micro jets formation and cavitation erosion.

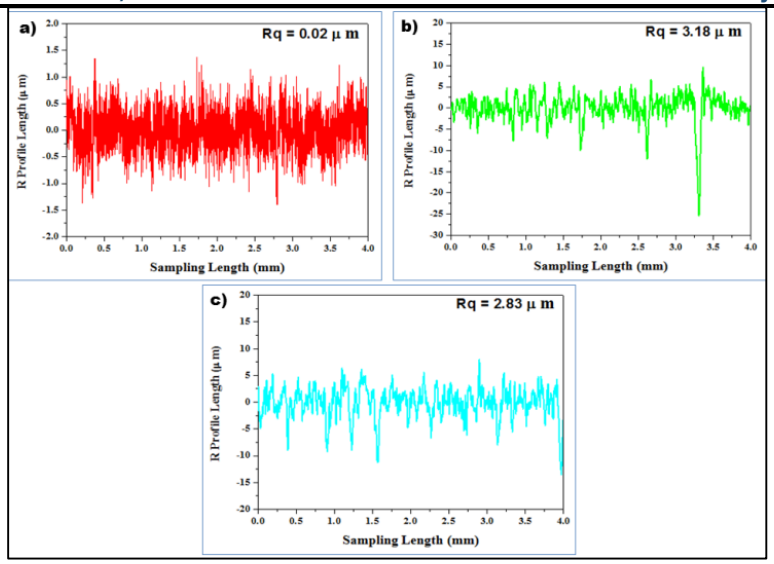

Fig. 8: Specimens Measured roughness profiles (a) Before Cavitation Testing (b) After Direct Cavitation Testing (c) After Indirect Cavitation Testing

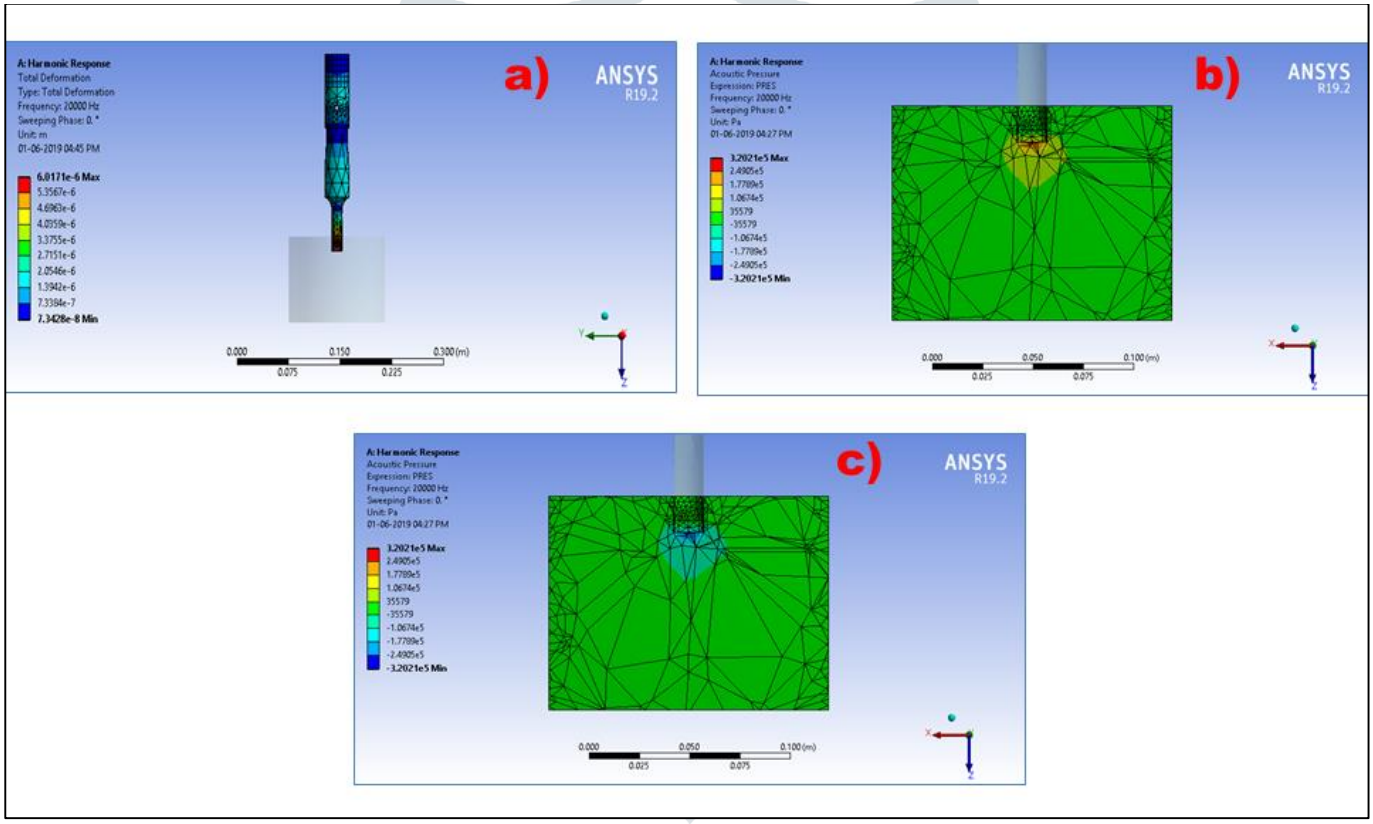

Fig. 9: Simulated results for direct acoustic cavitation testing in a 3-D volume of test liquid: (a) the displacement distribution in ultrasonic horn testing (b) the volumetric acoustic pressure distribution during upward movement of acoustic horn from its mean position (cut section view x-axis) (c) the volumetric acoustic pressure distribution during downward movement of acoustic horn from mean its position (cut section view x-axis)

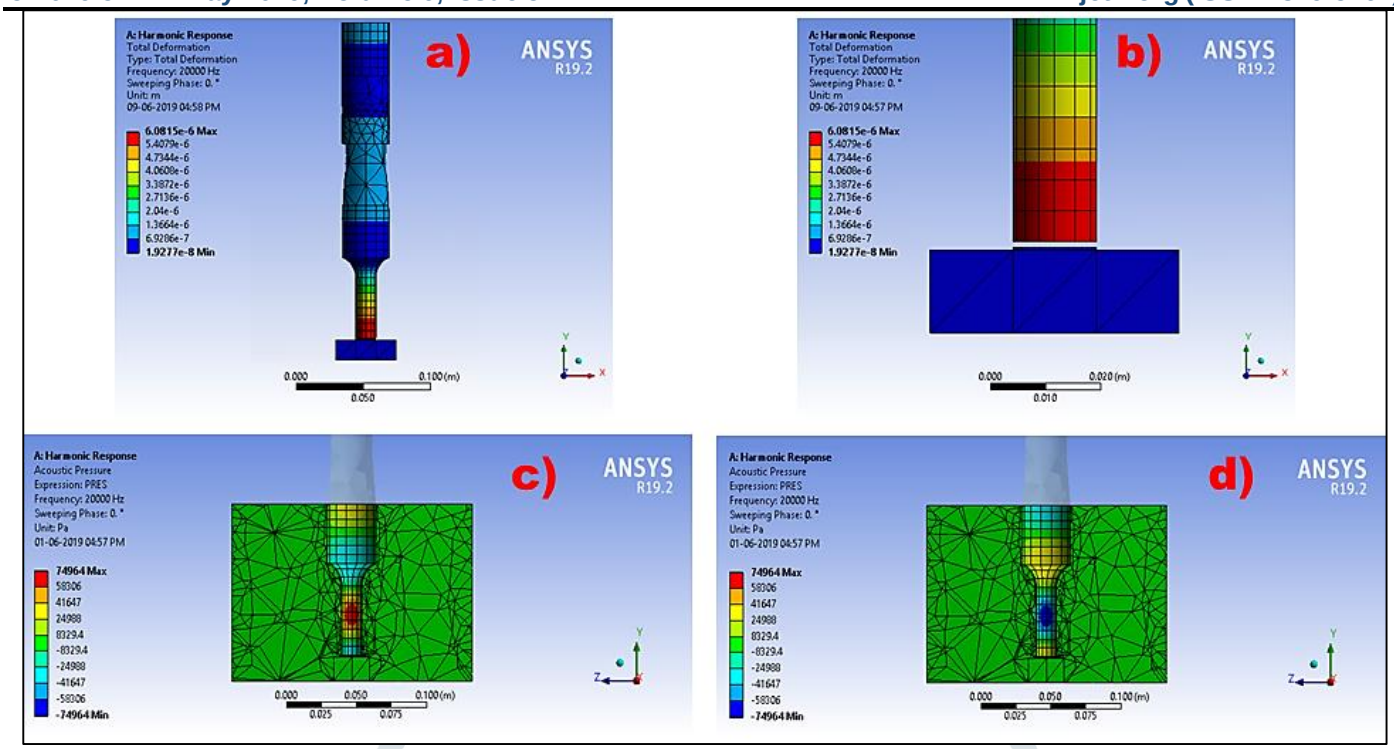

Fig.10: Simulated results for indirect acoustic cavitation testing in a 3-D volume of test liquid: (a) the displacement distribution in ultrasonic horn testing (b) enlarged view of ultrasonic horn (c) the volumetric acoustic pressure distribution during upward movement of acoustic horn from its mean position (cut section view z-axis) (d) the volumetric acoustic pressure distribution during downward movement of acoustic horn from mean its position (cut section view z-axis)

IV. CONCLUSION

In the present investigation, experimental and simulation studies of cavitation erosion and acoustic pressure in direct and indirect vibratory cavitation testing of the austenitic stainless steel 316 have been performed at 20 kHz vibration frequency and 60µm amplitude for 180 minutes on vibratory cavitation apparatus (probe sonicator). The major conclusions drawn are:

1. The cavitation erosion study reveals that the cumulative volume loss after direct vibratory cavitation testing is 3 times more than direct vibratory cavitation testing.
2. In the fracture analysis via SEM shows that a large number of deep craters, pits, micro cracks formation was responsible for the more volume loss in direct vibratory cavitation testing.
3. Mean square roughness value (Rq) after direct and indirect vibratory cavitation testing are 3.18µm and 2.83µm, respectively.
4. The maximum and minimum pressure in the direct method is 320210 Pa and -320210 Pa, respectively. And the maximum and minimum pressure in the indirect method is 74964 Pa and -74964 Pa, respectively. The acoustic pressure is approximately four times more while using the direct method.

ACKNOWLEDGMENT

The authors are very thankful to SERB (Science & Engineering research board), India, for the development of the following facilities: Probe sonicator & Optical Microscope with an image analyzer. Under the project titled “Development of Microwave Processed Cavitation Resistant Cladding” (Grant No. EMR/2016/007964).

REFERENCES

[1] S. Li, Tiny Bubbles Challenge Giant Turbines: Three Gorges Puzzle, Interface Focus. 5 (2015) 1–25.
[2] B.K. Sreedhar, S.K. Albert, A.B. Pandit, Cavitation Damage: Theory and measurements – A Review, Wear. 372–373 (2017) 177–196.
[3] A. Kumar, K. Govil, G. Dwivedi, M. Chhabra, Problems Associated with Hydraulic Turbines, In: Adv. Intell. Syst. Comput., Springer Singapore, (2018) 621–632.
[4] U. Dorji, R. Ghomashchi, Hydro Turbine Failure Mechanisms: An Overview, Eng. Fail. Anal. 44 (2014) 136–147.
[5] X. Liu, Y. Luo, Z. Wang, A Review on Fatigue Damage Mechanism in Hydro Turbines, Renew. Sustain. Energy Rev. 54 (2016) 1–14.
[6] R. Singh, S.K. Tiwari, S.K. Mishra, Cavitation Erosion in Hydraulic Turbine Components and Mitigation by Coatings: Current Status and Future Needs, J. Mater. Eng. Perform. 21 (2012) 1539–1551.
[7] A.K. Krella, D.E. Zakrzewska, Cavitation Erosion – Phenomenon and Test Rigs, Adv. Mater. Sci. 18 (2018) 15–26.
[8] X. Escaler, E. Egusquiza, M. Farhat, Detection of Cavitation in Hydraulic Turbines, Mech. Syst. Signal Process. 20 (2006) 983–1007.
[9] G.L. Chahine, J. Franc, A. Karimi, Laboratory Testing Methods of Cavitation Erosion, In: Adv. Exp. Numer. Tech. Cavitation Eros. Predict. (2014) 21–37.

[10] H.J. Amarendra, M.S. Pratap, S. Karthik, M.S. Punitha Kumara, H.C. Rajath, H. Ranjith, S. V Shubhatunga, Combined Slurry And Cavitation Erosion Resistance Of Surface Modified SS410 Stainless Steel, Mater. Sci. Eng. 330. 330 (2018) 1–7.

[11] L. Coleman, V.D. Scott, B. McEnaney, B. Angel, K.R. Stokes, Comparison of Tunnel and Jet Methods for Cavitation Erosion Testing, Wear. 184 (1995) 73–81.

[12] M. Riondet, G.L. Chahine, Impact Load Measurements in an Erosive Cavitating Flow, J. Fluids Eng. 133 (2011) 1–8.

[13] ASTM G32-16, Standard Test Method for Cavitation Erosion Using Vibratory Apparatus, ASTM International, West Conshohocken, PA, 2016.

[14] ASTM G134-17, Standard Test Method for Erosion of Solid Materials by Cavitating Liquid Jet, ASTM International, West Conshohocken, PA, 2017.

[15] K.Y. Chiu, F.T. Cheng, H.C. Man, Laser Cladding Of Austenitic Stainless Steel Using NiTi Strips for Resisting Cavitation Erosion, Surf. Coat. Technol. 402 (2005) 126–134.

[16] Y. Wang, J. Liu, N. Kang, G. Darut, T. Poirier, J. Stella, H. Liao, M. Planche, Cavitation Erosion of Plasma-Sprayed CoMoCrSi Coatings, Tribology Int. 102 (2016) 429–435.

[17] J.F. Santa, L.A. Espitia, J.A. Blanco, S.A. Romo, A. Toro, Slurry and Cavitation Erosion Resistance of Thermal Spray Coatings, Wear. 267 (2009) 160–167.

[18] L. Bai, W. Xu, J. Deng, C. Li, D. Xu, Y. Gao, Generation and Control Of acoustic Cavitation Structure, Ultrasonic Sonochemistry. 21 (2014) 1696–1706.

[19] S. Momeni, W. Tillmann, M. Pohl, Composite Cavitation Resistant PVD Coatings Based on NiTi Thin Films, JMADE. 110 (2016) 830–838.

[20] R. Singh, D. Kumar, S.K. Mishra, S.K. Tiwari, Laser Cladding of Stellite 6 on Stainless Steel to Enhance Solid Particle Erosion and Cavitation Resistance, Surf. Coatings Technol. 251 (2014) 87–97.

[21] C.L. Wu, S. Zhang, C.H. Zhang, H. Zhang, S.Y. Dong, Phase Evolution and Cavitation Erosion-Corrosion Behavior Of $FeCoCrAlNiTi_X$ High Entropy Alloy Coatings on 304 Stainless Steel by Laser Surface Alloying, J. Alloys Compd. 698 (2017) 761–770.

[22] X. Ding, X.C.C. Yuan, J. Shi, Structure of Micro-Nano WC-10Co4Cr Coating and Cavitation Erosion Resistance in NaCl Solution, Chinese J. Mech. Eng. 30 (2017) 1239–1247.

[23] Z.B. Zheng, Y.G. Zheng, W.H. Sun, J.Q. Wang, Effect of Heat Treatment on the Structure, Cavitation Erosion and Erosion-Corrosion Behavior Of Fe-Based Amorphous Coatings, Tribology Int. 90 (2015) 393–403.

[24] I. Hansoon, K. Aage, The Dynamics of Cavity Clusters in Ultrasonic (Vibratory) Cavitation Erosion, J. Appl. Phys. 51 (1980) 4651–4658.

[25] A. Arbor, G. Hammitt, Effect of Separation Distance on Cavitation Erosion of Vibratory and Stationary Specimens: In A Vibratory Facility, Wear. 102 (1985) 211–225.

[26] I. Ibanez, M. Hodnett, B. Zeqiri, M.N. Frota, Correlating Inertial Acoustic Cavitation Emissions with Material Erosion Resistance, Phys. Procedia. 87 (2016) 16–23.

[27] I. Tzanakis, G.S.B. Lebon, D.G. Eskin, K.A. Pericleous, Characterizing the Cavitation Development and Acoustic Spectrum in Various Liquids, Ultrasonic Sonochemistry. 34 (2017) 651–662.

[28] I. Lazar, I. Bordeasu, M.O. Popoviciu, I. Mitelea, T. Bena, L.M. Micu, Considerations Regarding the Erosion Mechanism of Vibratory Cavitation, Mater. Sci. Eng. 393 (2018) 1–8.

[29] P. Vatsh, K. Sahu, Testing Methods of Cavitation Erosion and the Impact of Component Material Selection on Pump Reliability, Int. J. Sci. Res. Dev. 5 (2017) 815–823.

[30] M.S. Vohra, N.A. Prasanth, W.L. Tan, S.H. Yeo, Analysis of Impact Load Induced by Ultrasonic Cavitation Bubble Collapse Using Thin Film Pressure Sensors, Int. J. Mech. Ind. Eng. 11 (2017) 1815–1820.

[31] S. Singh, J. Choi, G.L. Chahine, Characterization Of Cavitation Fields From Measured Pressure Signals Of Cavitating Jets And Ultrasonic Horns, J. Fluids Eng. 135 (2013) 1–11.

[32] A. Lichtarowicz, A Study Of Pressures And Erosion Produced By Collapsing Cavitation, Wear. 186187 (1995) 425–436.

[33] J. Choi, G.L. Chahine, Relationship between Material Pitting and Cavitation Field Impulsive Pressures, Wear. 352–353 (2016) 42–53.

[34] J.R. Laguna-Camacho, R. Lewis, M. Vite-Torres, J.V. Mendez-Mendez, A Study of Cavitation Erosion on Engineering Materials, Wear. 301 (2013) 467–476.

[35] ASTM E112-13, Standard Test Methods for Determining Average Grain Size, ASTM International, West Conshohocken, PA, 2013.

[36] Y. Tian, Z. Liu, X. Li, L. Zhang, R. Li, R. Jiang, F. Dong, The Cavitation Erosion Of Ultrasonic Sonotrode During Large-Scale Metallic Casting: Experiment And Simulation, Ultrasonics - Sonochemistry. 43 (2018) 29–37.